

# Safety of Multi-channel Stimulation Implants:

## Are Blocking Capacitors Sufficient After Single-Fault Failure?

Antoine Nonclercq, *Member, IEEE*, Laurent Lony, Anne Vanhoestenberghe, Andreas

Demosthenous, *Senior Member, IEEE*, and Nick Donaldson

**Abstract**— One reason given for placing capacitors in series with stimulation electrodes is that they prevent direct current flow and therefore tissue damage under fault conditions. We show that this is not true for multiplexed multi-channel stimulators with one capacitor per channel. A test bench of two stimulation channels, two stimulation tripole and a saline bath was used to measure the direct current flowing through the electrodes under fault conditions. The electrodes were passively discharged between stimulation pulses. For the particular condition used (16mA, 1ms stimulation pulse at 20Hz with electrodes placed 5cm apart), the current ranged from 38 $\mu$ A to 326 $\mu$ A depending on the type of fault. Variation of the fault current with time, stimulation amplitude, stimulation frequency and distance between the electrodes is given. Possible additional methods to improve safety are discussed.

**Index Terms**— Blocking capacitor, Functional Electrical Stimulation (FES), fault current, safety, tissue damage, electrodes.

### I. Introduction

Implanted neuroprostheses allow patients suffering from neural impairments to recover functionality lost as a result of an injury or disease. There are many examples of successful neuroprosthetic devices including cardiac pacemakers, cochlear implants, bladder control implants and dropped foot stimulators. Safety must be assessed before new devices can be tested in patients, even for a pre-commercial trial, in order to obtain regulatory approval, and electrical safety should be given due consideration from the beginning of the electronic design work.

Direct Current (DC) flowing through electrodes is a major safety concern, as it may cause tissue damage [1], [2]. For example, it has been reported that DC levels as low as  $2-3\mu\text{A}$  cause pathological changes in rat spinal cords [1] or in cat auditory nerves [3]. Therefore, both the U.S. Food and Drug Administration (FDA) and E.U. 60601 harmonized standards limit the amount of DC during normal and single fault condition (such as a short-circuit fault in a semiconductor component). For instance, for E.U. active implantable medical devices, “no leakage current (direct current) of more than  $1\mu\text{A}$  shall be sustained in any of the current pathways when the device is in use” [4]. The mechanisms for stimulation induced tissue damage are not well understood [2]. However, three hypotheses have been proposed: intrinsic biological processes as excitable tissue is over-stimulated (mass action theory) [5], toxic electrochemical reaction products at the electrode surface [6] and electroporation [7].

A typical way to limit DC is the use of blocking capacitor connected in series with the electrodes. Blocking capacitors have two additional benefits: they ensure that no charge accumulates on the electrodes and they allow “slide back” of the operating potential range of the electrodes so that it tends to remain within the “water window” [8], [9]. When there is only one stimulation channel or when every stimulation channel is electrically isolated by having an independent [power supply](#) [inductive link](#) (as is [3]), the blocking capacitors indeed ensure low levels of DC even during single fault conditions. Usually, however, multi-channel stimulators now use multiplexing and a common power supply (e.g. [9]) so the stimulation channels are not isolated from each other. In that case, despite having blocking capacitors on every channel, there is a possibility that DC may flow between neighboring channels. This paper explores the effect of short-circuit failures in the stimulator output stage, quantifies the resulting DC and proposes methods of prevention.

## II. Methods

A specially-made two-channel stimulator was used to measure DC at the electrodes under short-circuit fault conditions. Each channel was connected to a platinum tripole in the slot of an electrode book [10] immersed in a bath of isotonic saline (9 grams of NaCl per liter). The books were placed

[close together](#) ( $5\text{cm}$  apart, unless otherwise noted), [corresponding to a worst-case scenario](#). An

**Commentaire [AD1]:** How was this value chosen ?

ammeter (described below) was used to measure DC flowing from and to the electrodes, one at a time.

This section describes the circuits used and shows typical waveforms illustrating normal functioning.

### **Stimulator circuit**

An output stage of a type used by our team [9] was chosen for this study. It generates a charged-balanced biphasic stimulating current by active charging and floating passive discharge [11]. Fig. 1 shows the basic circuit (one channel only). During stimulation, the anode switch ( $S_a$ ) is closed, the discharge switch ( $S_d$ ) is open and the current sink (CS) is turned on. During discharge,  $S_d$  is closed,  $S_a$  is open and the current sink is turned off. The electrodes that are called ‘anode’ (A) and ‘cathode’ (K) are respectively positively and negatively polarized *during the stimulation current pulses*. A 20V power supply voltage ( $V_{dd}$ ), a  $2.5\text{k}\Omega$  discharge resistor ( $R_d$ ) and a  $4.7\mu\text{F}$  blocking capacitor ( $C_b$ ) were chosen to replicate a typical stimulator. The amplitude of the current sink can be set to 4mA, 8mA or 16mA (in this paper, an amplitude of 16mA was used on Ch 1 unless otherwise noted, and it was always 16mA on Ch 2). The output impedance of the current sink was  $134\text{k}\Omega$  when turned on and above  $100\text{M}\Omega$  otherwise.

Stimulation pulses were of 1ms duration and outputs were pulsed alternately at 20Hz (unless otherwise noted). A microcontroller was used to synchronize both channels: at time  $t_0$  Ch 1 stimulates for 1ms; at time  $t_0 + 25\text{ms}$  Ch 2 stimulates for 1ms; at time  $t_0 + 50\text{ms}$  the cycle starts again. Manual switches in parallel with the anode switch ( $S_a$ ) and with the current sink on Ch 2 allow short circuiting one of those components to simulate a fault. Those two faults were identified as the most critical as they link the power rail or the  $V_{ss}$  to the electrode (directly or via the blocking capacitor in the case of the current sink).

**Commentaire [A2]:** “Should we quote the capacitor type ? E.g., tantalum”

Ceramic capacitors were used. I do not think the capacitor type has an impact on the results. I think it would be better not to quote the capacitor type as otherwise we may have to justify our choice (Why not tantalum? What is the impact? ...) which may be too long to explain in this paper.

**Commentaire [A3]:** “I would be useful to say was the current sink constructed and its output resistance ?”

I added the output impedance of the CS in the text.

I think it would be too long to explain how I measured it and how the CS was constructed. FYI, I added this information in the “Answers to Andreas comments” document.

### **DC ammeter**

DCs through the electrodes were recorded with an ammeter (Fig. 2) which was inserted in series with either  $A_1$  or  $A_2$ . The input impedance is formed by a  $50\mu\text{F}$  low-leakage polyester capacitor in parallel with a  $1\text{k}\Omega$  resistor. The current waveform is low-pass filtered by the combined resistance and

capacitance and the DC is the measured average voltage divided by the resistance. The input voltage is buffered by a FET-input instrumentation amplifier ([Texas Instruments INA116](#)) with low bias and offset currents (less than 100fA) and filtered with a 1Hz second order low-pass Sallen-Key filter. The output voltage is measured using a digital voltmeter (Fluke 76). The whole system (amplifier, filter and voltmeter) is battery-powered, avoiding this way any connection to mains and therefore minimizing the impact of the ammeter on the setup. The method was adapted from [12], [13]. The ammeter was calibrated (gain and offset) using a linear regression model, obtained by applying known DCs (20 measures, ranging from -20 $\mu$ A to 20 $\mu$ A) at its inputs. The average error between the linear regression model and the measures varies from 64nA for a  $\pm 20\mu$ A range to 3.3 $\mu$ A for a  $\pm 2$ mA range.

**Commentaire [AD4]:** Componet part and manufacturer ?

#### **Typical waveforms**

The setup was tested under normal conditions (no fault, all manual switches are open). For each channel, oscilloscope probes were placed at the anode and cathode, and a 47 $\Omega$  resistor was placed in series with the blocking capacitor. Current flowing in the cathode was deduced from the voltage drop across the resistor. Fig. 3 shows the resulting current and voltage waveforms. When neither tripole is active, the impedance between all of the electrodes and the power rails is [very high \(above 100M \$\Omega\$ \)](#).

**Commentaire [AD5]:** What number ?

The oscilloscope probes have impedance to ground, and when placing the probe on a floating channel, its impedance is placed in parallel to it. Thus, when there is no stimulation, the potentials return to zero pulled down by the [probe impedance \(1M \$\Omega\$  in parallel with 95pF\)](#). During stimulation of Ch 1, the active anode voltage is close to the positive supply rail and the cathode potential is determined by the interelectrode impedance (Fig. 3 left). Because Ch 2 is floating at this time, the anode and cathode follow the potential imposed by Ch 1 (between Ch 1 anode and cathode voltages), as seen in Fig. 3 (right). When a channel is discharging, a small discharge current flows from the cathode to the anode, and the potential at the cathode becomes slightly higher than that of the anode. When stimulating with the nominal parameters (electrodes placed 5cm apart, stimulating at 20Hz and 16mA) an average DC of 104nA was measured with 22nA standard deviation over 20 measurements. Leakage DC is therefore low (and close to the average linear error of the ammeter) under normal conditions.

**Commentaire [AD6]:** We should quote the probe impedance. E.g., 10MOhm//10pF

### III. Results

This section compares the system under normal then single fault condition, respectively for a current sink short-circuit then an anode switch ( $S_a$ ) short-circuit in Ch 2. DCs at the electrodes are measured 60 seconds after the fault has occurred, leaving time for the stimulating system, the electrodes voltage and the DC measurement to stabilize.

#### ***Current sink failure***

Figure 4 explains how current flows during the stimulation and discharge periods of Ch 1. When stimulating, a 16mA pulse flows from the anode switch ( $S_{a1}$ ) to the current sink ( $S_1$ ), as required. However, because of the short-circuit across  $S_2$ , a large current flows from  $S_{a1}$  to the cathode of the faulty channel ( $K_2$ ) at the same time, charging up the capacitor  $C_{b2}$ . This current is determined mainly by the impedance between  $A_1$  and  $K_2$ . A smaller current also flows from  $A_1$  to  $A_2$  and then via  $S_{d2}$  to  $V_{ss}$ . During the discharge period of Ch 1, Ch 1 is floating so that  $C_{b2}$  can only discharge via  $A_2$ . Because an instantaneous fault current flows from  $A_1$  during stimulation but does not come back through it during the discharge period, there is an average current (i.e., DC) flowing at  $A_1$ . The blocking capacitors ensure that DC at the cathodes ( $K_1$  and  $K_2$ ) is zero. As a result the amount of DC flowing from  $A_1$  equals the amount of DC flowing to  $A_2$ :

$$I_{DC} = \frac{1}{T_{S1} + T_{D1}} \int I_{CS} \cdot dt \quad (1)$$

where,

- $I_{DC}$  is the DC at  $A_1$  or  $A_2$ ,
- $T_{S1}$  is the stimulation period of Ch 1,
- $T_{D1}$  is the discharge period of Ch 1,
- $I_{CS}$  is the current flowing in the current sink of Ch 2.

The fault current is quantified in Eq. (1) for two electrodes. If more than two channels were in use, the fault current would come from more anodes, and hence be greater. During stimulation of Ch 2, the current delivered to its load is too large (above 16mA) since the current sink is short-circuited.

However, since Ch 1 is isolated, no current flows to it. Therefore this large pulse current does not influence the amount of DC (but may still be harmful).

Figure 5 shows the resulting current and voltage waveforms. In Ch 1 (left of the figure) the voltage drop between the anode and cathode is larger than in Fig. 3 because more than 16mA flows from the active anode. A current pulse is now seen on Ch 2 (right of the figure). Ch 2 anode and cathode are connected to  $V_{ss}$  (through the blocking capacitor for  $K_2$  and the discharge resistor for  $A_2$ ).

When stimulating with the nominal parameters (electrodes placed 5cm apart, stimulating at 20Hz and 16mA) an average DC of  $326\mu A$  was measured with  $2.26\mu A$  standard deviation over 20 measurements. Identical readings were taken from both anodes ( $A_1$  and  $A_2$ ), as expected (in the following, the measurements were taken at  $A_2$ ). Variations of the DC with time, stimulation amplitude, stimulation frequency and distance between the electrodes are shown in Fig. 6.

The measured DC fluctuates in a repeatable fashion over time (Fig. 6 a): slow decreases are followed by sudden increases. The slow decreases are due to bubbles forming over the electrode surface as a result of electrolysis. Periodically these float away (the arrows indicate each time a bubble came off), freeing the electrode surface, hence lowering the impedance and causing the jump in measured current. In this paper, the measurements are taken 60 seconds after initiating the fault to ensure a good reproducibility, because bubbles took much longer to form.

The DC decreases as the pulse amplitude of Ch 1 (with intact current sink) increases (Fig. 6 b). The fault current flows from  $A_1$  to the lower power rail via the shorted current sink of Ch 2. It is determined by the voltages at the electrodes of Ch 2 ( $A_2$  and  $K_2$ ). The voltage at  $A_2$  is equal to  $V_{dd}$  minus the voltage dropped from  $A_1$  to  $A_2$  at the electrodes and through the saline. Similarly, the voltage at  $K_2$  is equal to  $V_{dd}$  minus the voltage dropped from  $A_1$  to  $K_2$  at the electrodes and through the saline. During the stimulation pulse, the higher the stimulation current, the higher the voltage drops from  $A_1$  to both electrodes of Ch 2, the lower the fault current to the shorted current sink ( $CS_2$ ). The linear shape of the curve suggests that the impedance of the electrode and the solution is constant with current amplitude in the considered range.

The variation with stimulation frequency shows a linear behavior at low frequency, with saturation at higher frequencies (Fig. 6 c). From Eq. (1), if  $I_{CS}$  were constant, the DC variation with stimulation frequency should be linear, since the stimulation frequency is equal to  $1/(T_{S1} + T_{D1})$ . However, as the frequency increases, the blocking capacitor of the second channel does not have time to fully discharge and the fault current tends to saturate.

The variation with the distance between the electrodes shows a non-significant downward trend. This limited influence is expected as the solution has a relatively high conductivity and most of the voltage drop is likely to occur at the electrode interfaces and in the slots of the books.

#### **Anode switch failure**

Figure 7 shows the current flow during the stimulation and discharge periods of Ch 1 when the anode switch of Ch 2 is shorted. In this fault condition, the current is still controlled by the current sink of the active channel ( $CS_1$ ). However that current is now drawn from both anodes. During the discharge time,  $K_1$  and  $C_{b1}$  can only discharge through  $A_1$ . Because an instantaneous fault current flows from  $A_2$  during stimulation but does not come back through it during the discharge period, there is an average current (i.e., DC) flowing at  $A_2$ . Again, the blocking capacitors ensure that DC at the cathodes ( $K_1$  and  $K_2$ ) is zero and as a result the amount of DC flowing from  $A_2$  equals the amount of DC flowing to  $A_1$ :

$$I_{DC} = \frac{1}{T_{S1} + T_{D1}} \int_{T_{S1}} I_{Sa} \cdot dt \quad (2)$$

where  $I_{Sa}$  is the current flowing in the shorted anode switch of Ch 2; all the other terms are identical to the ones of Eq. (1). Note that, compared with the current sink fault the net DC now flows in the opposite direction.

Figure 8 shows the resulting current and voltage waveforms. The potential of the solution is pulled up to the power supply voltage since the anode of the second channel is connected to  $V_{dd}$ . Thus, when a channel is floating, both its electrodes are pulled up to that voltage. When Ch 1 is stimulating, a voltage drop is present between its anode and cathode (Fig., 8 left), because the stimulation current flows between them.

When stimulating with the nominal parameters (electrodes placed 5cm apart, stimulating at 20Hz and 16mA) an average DC of  $37.9\mu\text{A}$  was measured with  $0.57\mu\text{A}$  standard deviation over 20 measurements. Variation of the DC with time, stimulation amplitude, stimulation frequency and distance between the electrodes is shown in Fig. 9.

Once the fault is established, the DC decreases and tends to stabilize after about 90 minutes (Fig. 9 a). Here, electrolysis also occurs at the interface, but as the DC level is lower, smaller bubbles form which tend to come off more easily, so that equilibrium between bubble formation and detachment is quicker.

The DC increases as the pulse amplitude of Ch 1 (with intact anode switch) increases (Fig. 9 b). This should be expected since the fault current is determined by the amplitude of the current sink of the first channel ( $\text{CS}_1$ ) where it flows. The portion of current flowing into  $\text{CS}_1$  from each anode is determined by the impedance of the electrodes and solution. The linear shape of the curve suggests that it is constant with current amplitude in the considered range (similarly to what was observed in the case of current sink failure).

The variation with stimulation frequency shows quite a linear behavior (Fig. 9 c). From Eq. (2), this linear trend implies that the integral of  $I_{\text{sa}}$  is constant with frequency, since stimulation frequency is equal to  $1/(T_{\text{S}1} + T_{\text{D}1})$ . As  $I_{\text{sa}}$  is determined by the potential at  $A_2$  (kept constant at  $V_{\text{dd}}$ ), the current pulse amplitude (kept constant), and the impedance of the electrode and of the solution, it suggests that these impedances are relatively constant with frequency in the range considered.

The variation with the distance between the electrodes shows an insignificant downward trend. Again, this limited influence is expected as the solution has a relatively high conductivity and most of the voltage drop is likely to occur at the electrode interfaces and in the slots.

#### IV. Discussion and conclusions

The result of this study demonstrate that DCs may flow between the anodes in case of an anode switch failure – and more so in case of a current sink failure – even when using blocking capacitors at the cathodes. The DC is highly dependent on time, stimulation amplitude, and stimulation frequency

but not significantly on the distance between the electrodes. These levels of DC would most certainly lead to tissue damage as they are typically one or two orders of magnitude higher than the  $2\text{-}3\mu\text{A}$  level for which damage has already been seen [1], [3].

One way to avoid DC for both types of faults would be to add anode blocking capacitors for every channel. However, the extra space this will require is very disadvantageous. A second way would be to use multichannel systems formed from isolated single channels, as is the case for the BION [14], [15]. This approach may be attractive when there are several widely-separated stimulation sites or for systems requiring only few channels. However, it would be unsuitable for a large number of electrodes physically close to one another. A third way would be to monitor the voltage at a node of the circuit that is normally floating when the channel is isolated (e.g., the anode). A short-circuit on the current sink would be detected as the anode voltage would sink below a pre-agreed threshold during adjacent channel stimulation (because the anode would be pulled down by the short-circuit). Similarly, a short-circuit on the anode switch would be detected as the anode voltage would be constantly at  $V_{dd}$ . The difficulty with this would be the arbitrariness of any criterion used, given the undefined potential when there is no fault. A fourth way would be to monitor the voltage drop across the load, to estimate the current flowing in it and by this way ensure it is close to zero when not stimulating, as previously proposed [16]. This monitoring would require a differential amplifier [9], but would greatly increase the complexity of the circuit.

An alternative for current sink failure would be to monitor the current effectively drawn by the circuit by adding a current monitor at the power supply (common to all output stages). If the current drawn exceeds the current defined by the current sink by more than a small amount, a fault is detected and the implant deemed hazardous and switched off. A similar implementation has been previously proposed [16]. Regarding anode switch failure, independent switches at the anode (i.e., redundancy), as well as regular verification of the proper functioning of those switches would ensure the safety of the system.

Other types of failure than those proposed in this paper should also be assessed. For instance, a short circuit in the blocking capacitor might lead to high levels of DC. When blocking capacitors are not integrated, as is usually the case today, this type of failure is unlikely to occur. However, there have recently been developments to integrate blocking capacitors so as to reduce implant size [12] and these capacitors may be less reliable. ~~The possibility that the discharge switches ( $S_d$  in Fig. 1) fail open circuit should also be considered.~~

The conclusions from this study are that the use of single blocking capacitors in each stage of a multiplexed stimulator *does not* ensure that DC will not flow under single fault conditions. In fact with a plausible stimulation set-up, the fault current can be large enough to be dangerous. The designers of such stimulators that do use blocking capacitors should consider whether further precautions are desirable.

Many implants are developed by corporations and, due to their commercial nature, most of the development knowledge associated with them has remained confidential [14]. In particular, companies have no obligation to discuss the inevitable mistakes that have occurred along the development path. Whatever the topology used, implants such as pacemakers have been shown to produce high levels of DC when they fail [17], and hence may be dangerous for patients. We hope this study will help inform future design and promote safer implants.

## Acknowledgment

The authors thank Prof. Stéphane Godet and Benoit Haut for their help on this study.

**Commentaire [A7]:** "Why did not consider this for this paper ? Is that type of error likely to be less significant than the cases considered in this paper ?"

I did some measurements to assess this question and I added them in the "Answers to Andreas comments" document.

This fault differs from the others as no DC is involved. This way, it may be out of focus for this paper and rather belonging to the "Other types of failure than those proposed in this paper should also be assessed" sentence above. I would remove this sentence to avoid focusing the reviewers attention on this particular point.

## Bibliography

- [1] R. J. Hurlbert, C. H. Tator, and E. Theriault, "Dose-response study of the pathological effects of chronically applied direct current stimulation on the normal rat spinal cord," *J. Neurosurg.*, vol. 79, no. 6, pp. 905-16, Dec. 1993.
- [2] D. R. Merrill, M. Bikson, and J. G. R. Jefferys, "Electrical stimulation of excitable tissue: design of efficacious and safe protocols," *J. Neurosci. Methods.*, vol. 141, no. 2, pp. 171-98, Feb. 2005.
- [3] R. K. Shepherd, N. Linahan, J. Xu, G. M. Clark, and S. Araki, "Chronic electrical stimulation of the auditory nerve using non-charge-balanced stimuli," *Acta Otolaryngol.*, vol. 119, no. 6, pp. 674-84, Jan. 1999.
- [4] European Standard, "Part 1. EN45502-1 for safety, marking and information to be provided by the manufacturer," in *Active Implantable Medical Devices*, Brussels: CENELEC, 1998, p. 8.
- [5] W. F. Agnew, D. B. McCreery, T. G. Yuen, and L. a Bullara, "MK-801 protects against neuronal injury induced by electrical stimulation," *Neuroscience*, vol. 52, no. 1, pp. 45-53, Jan. 1993.
- [6] S. Brummer and M. Turner, "Electrical stimulation of the nervous system: The principle of safe charge injection with noble metal electrodes," *Bioelectrochem. Bioenerg.*, vol. 2, no. 1, pp. 13-25, 1975.
- [7] A. Butterwick, A. Vankov, P. Huie, Y. Freyvert, and D. Palanker, "Tissue damage by pulsed electrical stimulation," *IEEE Trans. Biomed. Eng.*, vol. 54, no. 12, pp. 2261-7, Dec. 2007.
- [8] N. de N. Donaldson and P. E. K. Donaldson, "When are actively balanced biphasic ('Lilly') stimulating pulses necessary in a neurological prosthesis? II pH changes; noxious products; electrode corrosion; discussion," *Med. Biol. Eng. Comput.*, vol. 24, no. 1, pp. 50-56, Jan. 1986.
- [9] P. J. Langlois, A. Demosthenous, I. Pachnis, and N. Donaldson, "High-power integrated stimulator output stages with floating discharge over a wide voltage range for nerve stimulation," *IEEE Trans. Biomed. Circuits Syst.*, vol. 4, no. 1, pp. 39-48, Feb. 2010.
- [10] Tripolar book electrodes, "Finetech Medical Ltd.," *13 Tewin Court, Welwyn Garden City, Hertfordshire, AL7 1AU, United Kingdom*.
- [11] A. Vanhoestenberghe, "Implanted devices: improved methods for nerve root stimulation," University College London, 2007.
- [12] X. Liu, A. Demosthenous, and N. Donaldson, "An integrated implantable stimulator that is fail-safe without off-chip blocking-capacitors," *IEEE Trans. Biomed. Circuits Syst.*, vol. 2, no. 3, pp. 231-44, Sep. 2008.
- [13] C. Q. Huang, R. K. Shepherd, P. M. Carter, P. M. Seligman, and B. Tabor, "Electrical stimulation of the auditory nerve: direct current measurement in vivo," *IEEE Trans. Biomed. Eng.*, vol. 46, no. 4, pp. 461-70, Apr. 1999.

- [14] M. J. Kane, P. P. Breen, F. Quondamatteo, and G. ÓLaighin, "BION microstimulators: a case study in the engineering of an electronic implantable medical device," *Med. Eng. Phys.*, vol. 33, no. 1, pp. 7-16, Jan. 2011.
- [15] G. E. Loeb, R. a Peck, W. H. Moore, and K. Hood, "BION system for distributed neural prosthetic interfaces," *Med. Eng. Phys.*, vol. 23, no. 1, pp. 9-18, Jan. 2001.
- [16] M. Ortmanns, A. Rocke, M. Gehrke, and H.-Jü. Tiedtke, "A 232-Channel Epiretinal Stimulator ASIC," *IEEE J. Solid-State Circuits*, vol. 42, no. 12, pp. 2946-59, Dec. 2007.
- [17] J. D. Fisher, S. Furman, B. Parker, and D. J. Escher, "Pacemaker failures characterized by continuous direct current leakage," *Am. J. Cardiol.*, vol. 37, no. 7, pp. 1019-23, Jun. 1976.

## **Figure captions**

Fig. 1 - One stimulation channel. The stimulation tripole is within the slot of a silicone rubber *book* [10] which is represented by the dashed rectangle.

Fig. 2 – Floating DC ammeter.

Fig. 3 – Current and voltage waveforms during normal operation (no fault) about the time of the stimulating pulse on Ch 1. Ch 2 remains in its discharging state in this period. Left: measured current at  $K_1$  and voltages at the electrodes on Ch 1. Right: measured current at  $K_2$  and voltages at the electrodes on Ch 2.

Fig. 4 – Current sink failure: current flowing during Ch 1 stimulation (left) and discharge (right). Currents expected under normal conditions are shown with plain lines and currents due to the fault are shown with dashed lines.

Fig. 5 – Current and voltage waveforms during current sink failure. Format same as Fig. 3.

Fig. 6 – Current sink failure: variation of the DC with time (top left), stimulation amplitude (top right), stimulation frequency (bottom left) and distance (bottom right).

Fig. 7 – Anode switch failure: current flowing during Ch 1 stimulation (left) and discharge (right). Currents expected under normal conditions are shown with plain lines and currents due to the fault are shown with dashed lines.

Fig. 8 – Current and voltage waveforms during anode switch failure. Format same as Fig. 3.

Fig. 9 – Anode switch failure: variation of the DC with time (top left), stimulation amplitude (top right), stimulation frequency (bottom left) and distance (bottom right).

## Figures

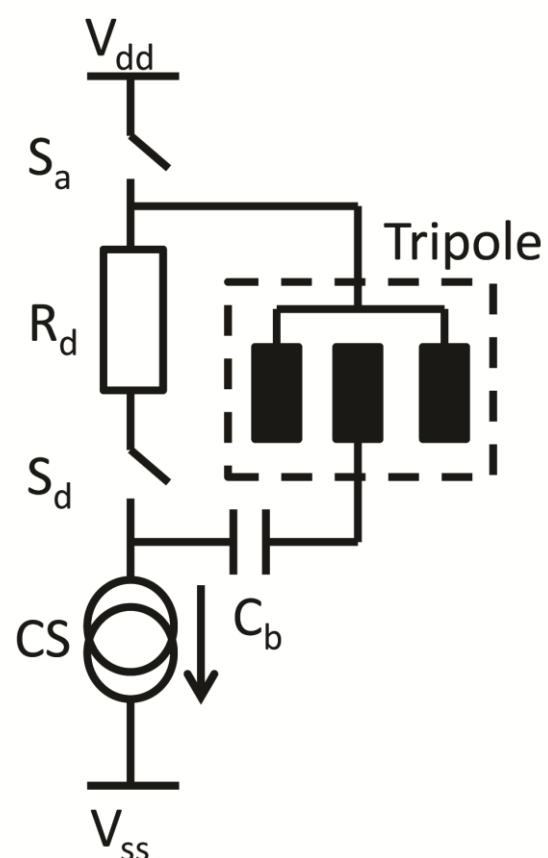


Figure 1.

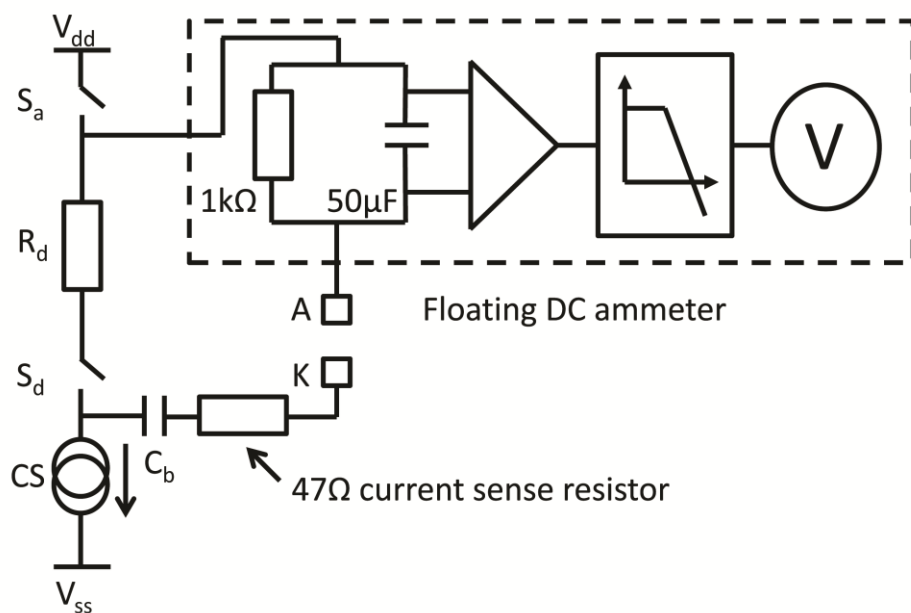


Figure 2.

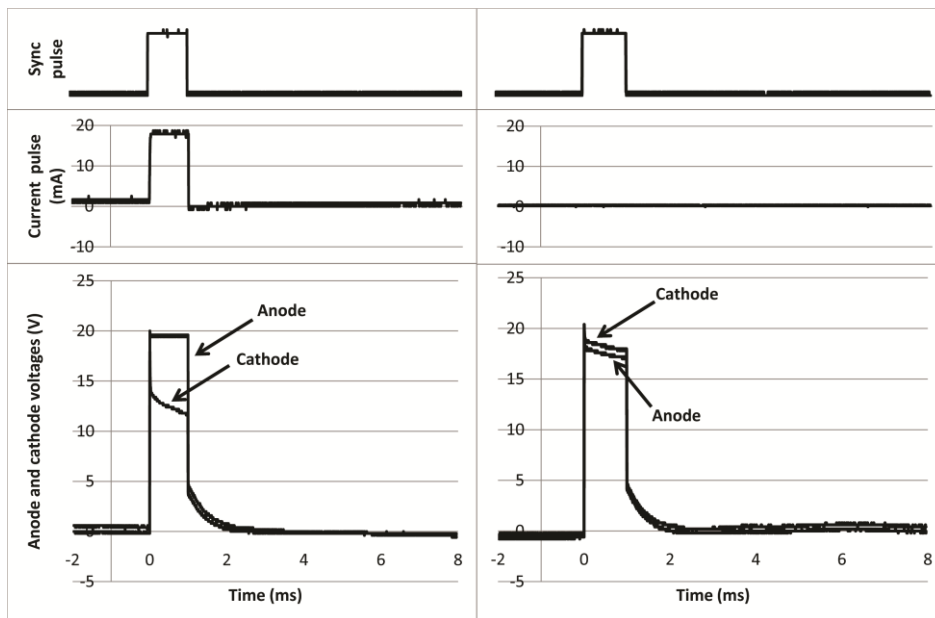


Figure 3.

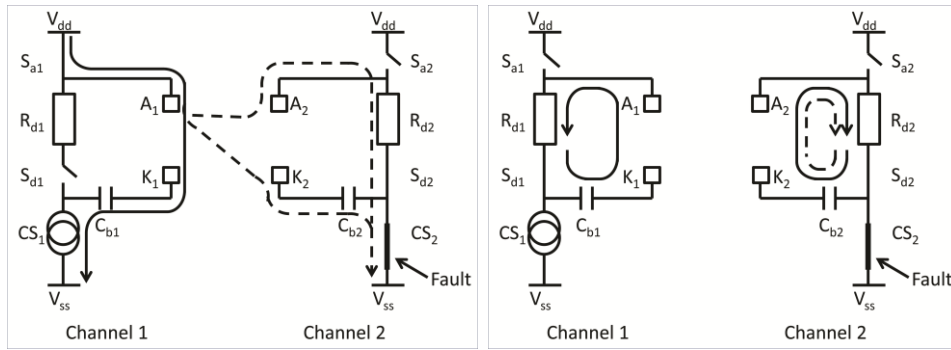


Figure 4.

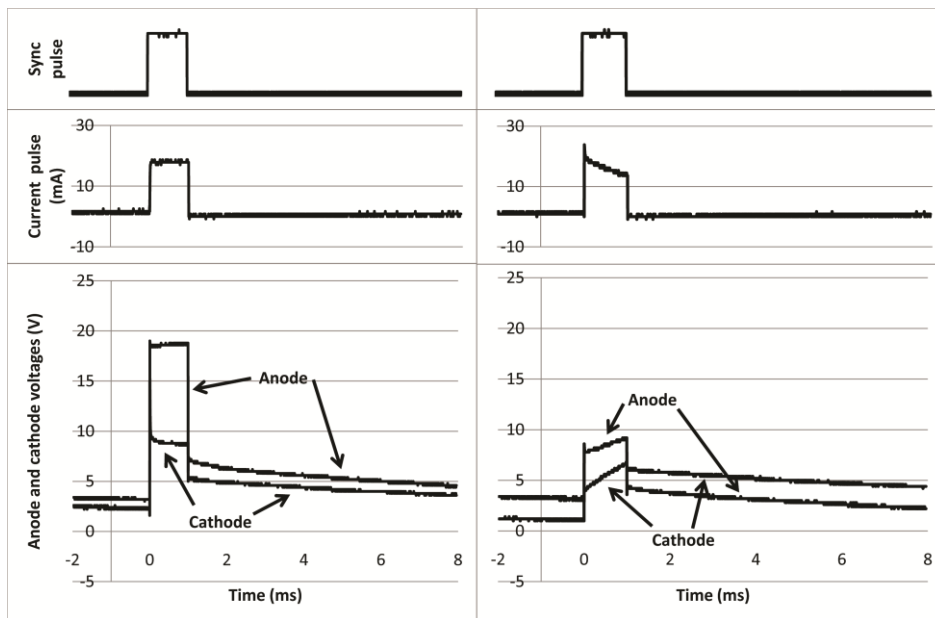


Figure 5.

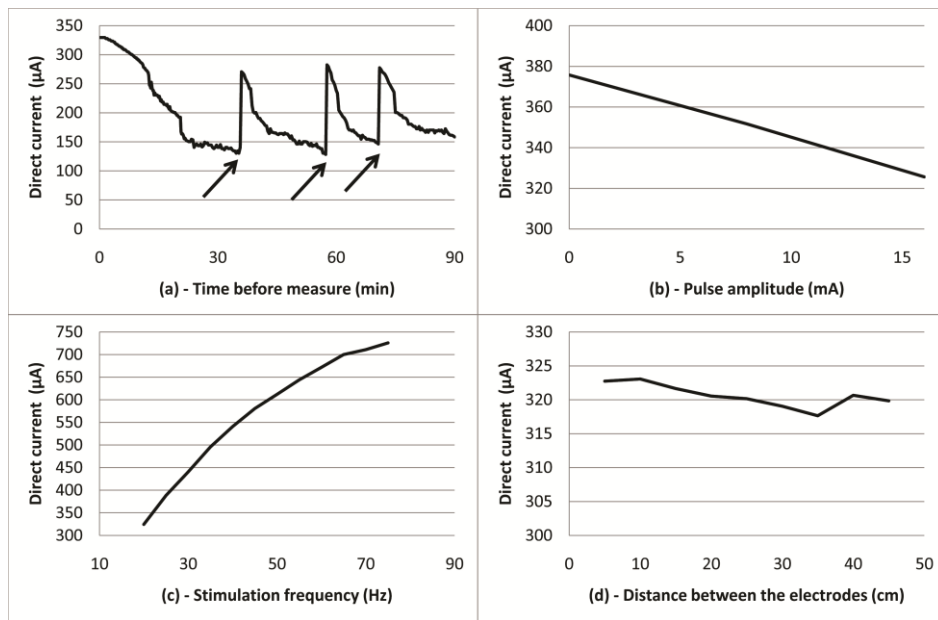


Figure 6.

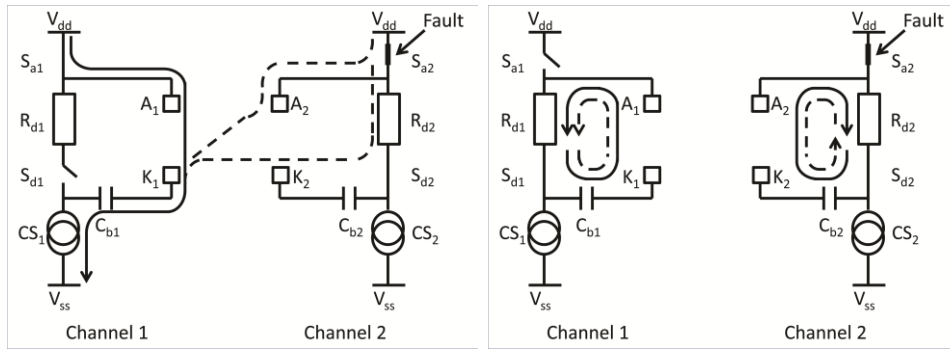


Figure 7.

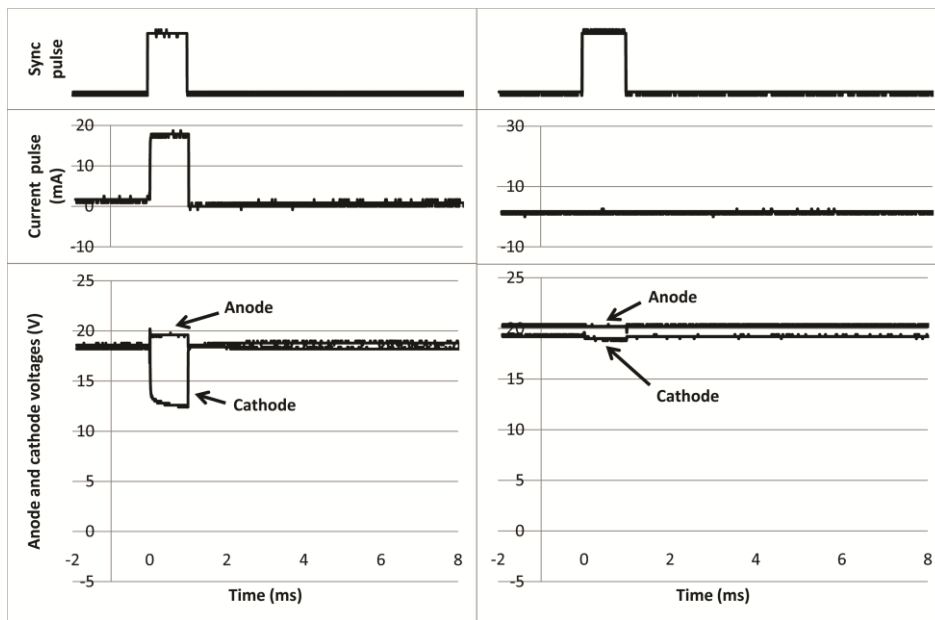


Figure 8.

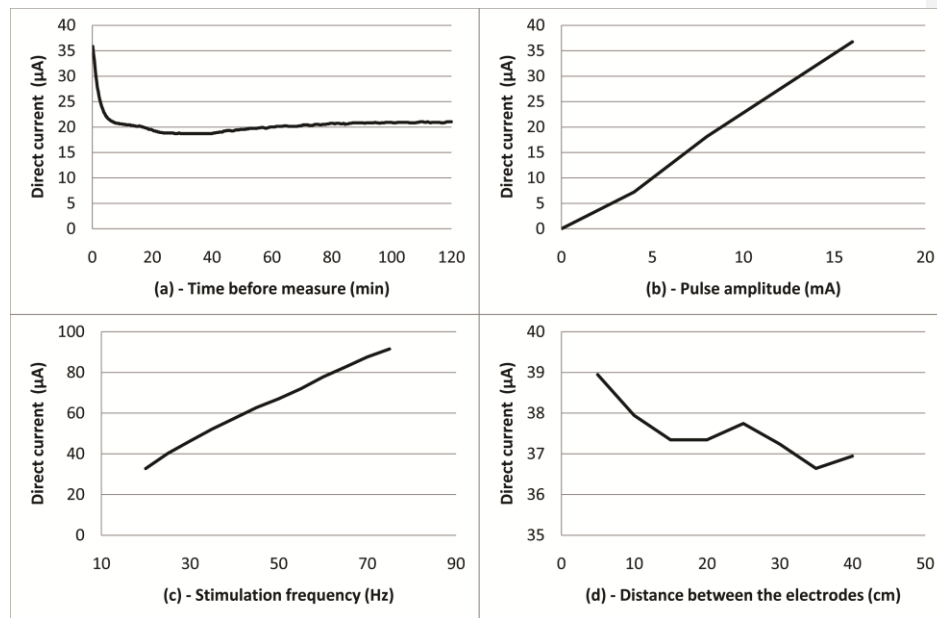


Figure 9.